

# Theoretical investigations of temperature-compensated cuts for vibrating beam LGT resonators

F. Sthal, E. Bigler and R. Bourquin  
FEMTO-ST Institute, UMR CNRS 6174  
ENSM  
Besançon, France  
fsthal@ens2m.fr

**Abstract—** In this paper, the possibility of temperature-compensated cuts for different kinds of vibrations in Langatate resonators is investigated. Theoretical investigations of vibrating beam resonators with a rectangular cross-section in extensional, flexural and torsional modes are given.

## I. INTRODUCTION

Lanthanum gallium tantalate (langatate - LGT) is a synthetic crystal grown by means of Czochralski method [1-4]. LGT crystal class is 32 which is the same than quartz crystal. Its chemical composition is  $\text{La}_3\text{Ga}_{5.5}\text{Ta}_{0.5}\text{O}_{14}$ . This crystal has certain advantages compared to traditional piezoelectric materials (quartz). LGT has no phase transitions up to the melting temperature 1450 °C, no pyroelectric effect. However the material demonstrates high electromechanical coupling factor (more than twice as much as quartz) and steady-state value of piezoelectric constant  $d_{11}$  in a temperature range up to 600 °C (less than 5% change up to 450 °C). This crystal begins to know bulk and surface acoustic wave applications [5-7]. However, this material is not very well known in term of elastic coefficients and thermal sensitivities [8-11].

Temperature-compensated cuts have been investigated theoretically for quartz,  $\text{GaPO}_4$  and LGS by analytical methods for three kinds of vibrations: length extension, flexion and torsion [12-15]. In this paper, modeling and measuring temperature effects in LGT vibrating beam resonators are reported. Beam definition is given in Fig. 1.

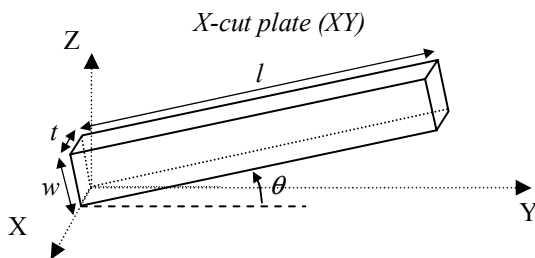


Figure 1. Beam orientations (X, Y, Z cristallographic axes).

Due to the unknown of the third order thermal coefficients of LGT, the temperature dependence of resonant frequencies is expressed by the parabolic equation:

$$f(T) = f(T_0) \left( 1 + T_f^{(1)}(T - T_0) + T_f^{(2)}(T - T_0)^2 \right) \quad (1)$$

where  $f$  is the frequency at the temperature  $T$ ,  $T_0$  is the reference temperature for which the elastic constants are defined and  $T_f^{(i)}$  (with  $i = 1, 2$ ) are the first two temperature coefficients of frequency (TCFs).  $T_0$  is set at 25 °C for all TCF calculus. Analytical expressions are obtained for both TCFs by means of a method which consists of varying the elastic constants, beam dimensions and mass density as a function of temperature.  $T_f^{(1)}$  and  $T_f^{(2)}$  are given for a beam oriented along the Y crystallographic axis (Fig. 1). Temperature compensated cuts exist in LGT for length extensional, flexural and torsional modes.

## II. LENGTH EXTENSIONAL MODE

The analytical model of length-extensional vibration is built without taking into account the piezoelectric effect [12]. It concerns rectangular cross-section beams. In this model, the length of the beam is assumed much greater than its width and its thickness. Resonant frequencies are determined from the equation of motion. For a free-free beam, we get:

$$f_n = \frac{n}{2 \cdot l} \frac{1}{\sqrt{\rho \cdot s_{22}}} \quad (2)$$

where  $n$  is a positive integer,  $l$  the length of the beam,  $\rho$  the mass density of material and  $s_{22}$  the compliance along the Y axis.

The thermal expansion coefficients used in this paper are given in [10]. By means of thermal expansion coefficients

$\alpha_{mm}^{(k)}$  (with  $k = 1, 2$  and  $mm = ww, ll, tt$ ) and thermal coefficients of compliances  $T_{Sij}^{(k)}$ , we have:

$$T_f^{(1)} = \frac{1}{2} (\alpha_{ww}^{(1)} + \alpha_{tt}^{(1)} - T_{s22}^{(1)} - \alpha_{ll}^{(1)}) \quad (3)$$

$$T_f^{(2)} = \frac{1}{4} \left[ 2\alpha_{ww}^{(2)} - (\alpha_{ww}^{(1)})^2 + 2\alpha_{tt}^{(2)} - (\alpha_{tt}^{(1)})^2 - 2T_{s22}^{(2)} + (T_{s22}^{(1)})^2 - 2\alpha_{ll}^{(2)} + (\alpha_{ll}^{(1)})^2 \right] + \frac{1}{2} (T_f^{(1)})^2 \quad (4)$$

Fig. 2 shows the first order temperature coefficient of frequency versus the rotation angle  $\theta$ . For LGT, two cut angles are found by means of coefficients published in [11].

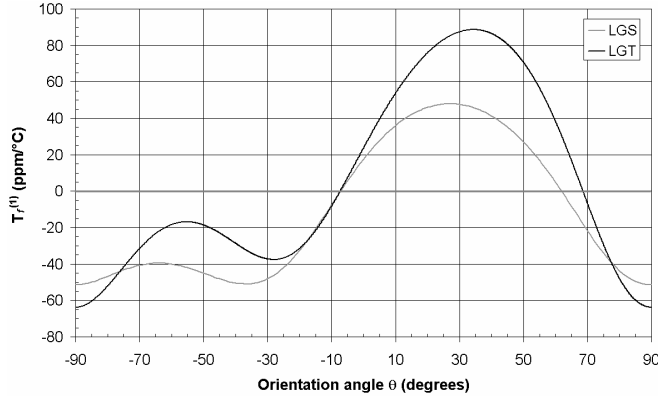


Figure 2.  $T_f^{(1)}$  versus rotation angle  $\theta$  for LGT and LGS.

Table 5 presents a comparison of the first order temperature compensated angles between Quartz, GaPO<sub>4</sub>, LGS and LGT crystals.

TABLE I. TEMPERATURE-COMPENSATED CUTS FOR RECTANGULAR BEAMS IN QUARTZ, GAPO<sub>4</sub>, LGS AND LGT: EXTENSIONAL MODE

| Rectangular beam      | Quartz [17]                          | GaPO <sub>4</sub> [18]                              | LGS [18]   | LGT [18]   |
|-----------------------|--------------------------------------|---|--|--|
| Length Extension (LE) | $\theta = 5^\circ$<br>(minimization) | $\theta = -8^\circ$<br>or<br>$\theta = -52.6^\circ$ | $\theta = -7^\circ$<br>or<br>$\theta = 62^\circ$ | $\theta = -7.3^\circ$<br>or<br>$\theta = 68.6^\circ$ |

Residual second order thermal coefficients of frequency are compared in Table 2. LGT, LGS and GAPO<sub>4</sub> have a similar behavior.

TABLE II. 2<sup>ND</sup> ORDER OF THERMAL COEFFICIENTS OF FREQUENCY FOR RECTANGULAR BEAM VIBRATING IN LENGTH EXTENSIONAL MODE.

|   | Quartz |        | GaPO <sub>4</sub> |           | LGS   |        |        | LGT      |          |
|---|--------|--------|-------------------|-----------|-------|--------|--------|----------|----------|
|   | BT cut | AT cut | LE -8°            | LE -52.6° | Y cut | LE -7° | LE 62° | LE -7.3° | LE 68.6° |
| $ T_f^{(2)} $<br>(10 <sup>-9</sup> /°C <sup>2</sup> ) | 40     | 20     | 7.5               | 1.4       | 50    | 53     | 129    | 83       | 102      |

The turn over point of the compensated cut can be moved between -200 °C to 250 °C. Fig. 3 shows the frequency-temperature behavior of LGT for three cut angles. To remark, GaPO<sub>4</sub> have temperature compensated cut up to 550 °C. For

LGS and LGT, the temperature limitation is probably due to the model which is only developed in second order.

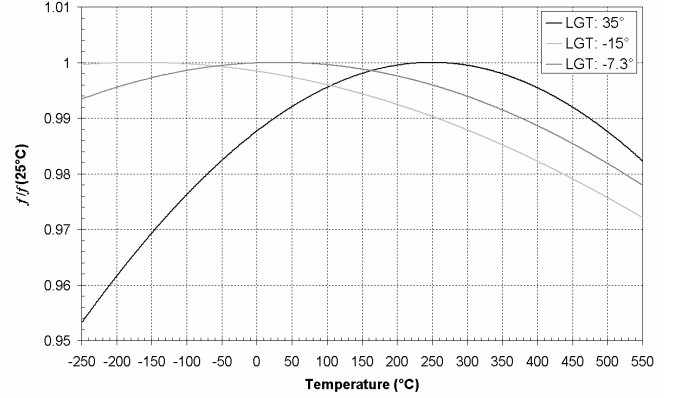


Figure 3. Normalized frequency versus temperature of LGT resonators for three rotation angle:  $\theta = 35^\circ$ ,  $\theta = -15^\circ$  and  $\theta = -7.3^\circ$ .

### III. FLEXURAL MODE

In the same way, a beam resonator vibrating in a flexural mode is studied. The derivation used in this model is based on the Bernoulli beam model where shear effects are neglected. These assumptions are valid when the beam length is much larger than its width and thickness. The resonant frequencies are:

$$f = \frac{\lambda^2}{2 \cdot \pi \cdot l^2} \sqrt{\frac{I}{s_{22} \rho S}} \quad (5)$$

with

$S$ : cross-sectional area of the beam

$s_{22}$ : Compliance for a beam oriented along the crystallographic Y-axis

$I$ : Inertia of beam with  $I = \frac{w \cdot t^3}{12}$

$\rho$ : mass density of material

$\lambda$  is solution of an eigenfrequency equation that depends upon the boundary conditions.

The first two TCFs  $T_f^{(i)}$  ( $i = 1, 2$ ) are given by:

$$T_f^{(1)} = \frac{1}{2} (\alpha_{ww}^{(1)} + 3\alpha_{tt}^{(1)} - T_{s22}^{(1)} - 3\alpha_{ll}^{(1)}) \quad (6)$$

$$T_f^{(2)} = \frac{1}{4} \left[ 2\alpha_{ww}^{(2)} - (\alpha_{ww}^{(1)})^2 + 6\alpha_{tt}^{(2)} - 3(\alpha_{tt}^{(1)})^2 - 2T_{s22}^{(2)} + (T_{s22}^{(1)})^2 - 6\alpha_{ll}^{(2)} + 3(\alpha_{ll}^{(1)})^2 \right] + \frac{1}{2} (T_f^{(1)})^2 \quad (7)$$

Fig. 4 shows the first TCF for LGS and LGT flexural mode resonators according to the rotation angle  $\theta$ .  $T_f^{(1)}$  for LGT crystal is equal to zero for two cut angles,  $\theta = -6.6^\circ$  and  $\theta = 69^\circ$ . LGT and LGS behaviors are very similar to extensional mode.

Table 3 presents the first order temperature compensated angles of LGT compared with quartz, GaPO<sub>4</sub> and LGS. Theoretical second order TCFs are given in table 4. LGS and LGT have a very similar behavior. GaPO<sub>4</sub> has a second order TCF smaller than LGT and LGS.

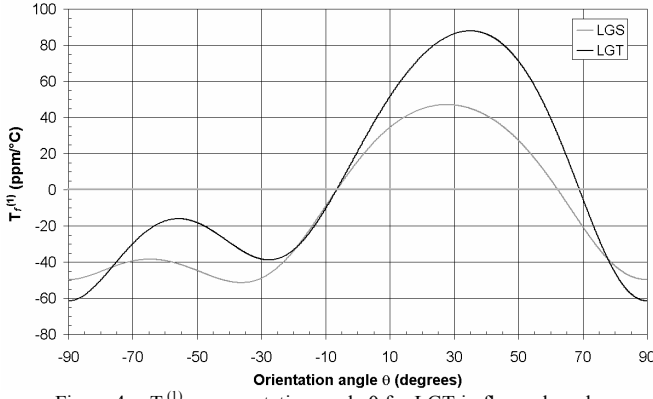


Figure 4.  $T_f^{(1)}$  versus rotation angle  $\theta$  for LGT in flexural mode.

TABLE III. TEMPERATURE-COMPENSATED CUTS FOR RECTANGULAR BEAMS IN QUARTZ, GAPO<sub>4</sub>, LGS AND LGT: FLEXURE

| Rectangular beam | Quartz [17]                          | GaPO <sub>4</sub> [18]                                 | LGS [18]   | LGT [18]   |
|------------------|--------------------------------------|--|--|--|
| flexion          | $\theta = 5^\circ$<br>(minimization) | $\theta = -14.1^\circ$<br>or<br>$\theta = -53.7^\circ$ | $\theta = -4^\circ$<br>or<br>$\theta = 60.3^\circ$ | $\theta = -6.6^\circ$<br>or<br>$\theta = 69^\circ$ |

TABLE IV. 2<sup>ND</sup> ORDER OF THERMAL COEFFICIENTS OF FREQUENCY FOR RECTANGULAR BEAM VIBRATING IN FLEXURAL MODE.

|                                      | GaPO <sub>4</sub> |        | LGS |       | LGT   |     |
|--------------------------------------|-------------------|--------|-----|-------|-------|-----|
| Flexion                              | -14.1°            | -53.7° | -4° | 60.3° | -6.6° | 69° |
| $ T_f^{(2)}  (10^{-9} / ^\circ C^2)$ | 8.5               | 2.8    | 57  | 127   | 87    | 99  |

In the same manner like for extensional mode, the temperature turnover point of the compensated cut can be moved from -200°C to 250°C.

#### IV. TORSIONAL MODE

The last beam resonator studied is vibrating beam in torsional modes. The resonant frequencies are determined by using the principle of energy's conservating. Hence, for a beam which is clamped-free, the resonant frequencies are [16]:

$$f = \frac{n}{4l} \sqrt{\frac{C_t}{\rho I_y}} \quad (8)$$

with

$I_y$ , the moment of inertia in rectangular cross-section,

$$I_y = \frac{tw(t^2 + w^2)}{12} \quad (9)$$

$C_t$ , the torsional constant.

$$C_t = \frac{C_{66} w^3 t}{3} \left( 1 - \frac{w}{t} \sqrt{\frac{C_{66}}{C_{44}}} 192 \dots \right. \quad (10)$$

$$\left. \dots \sum_{n=0}^{\infty} \frac{1}{(2n+1)^5} \pi^5 th \left( \frac{(2n+1)\pi}{2w} \sqrt{\frac{C_{44}}{C_{66}}} \right) \right)$$

The first TCF of torsional modes is given by:

$$T_f^{(1)} = -\alpha_{ll}^{(1)} + \frac{3}{2} \alpha_{ww}^{(1)} + \frac{1}{2} \alpha_{tt}^{(1)} + \frac{1}{2} T_{C_{66}}^{(1)} - \frac{t^2}{t^2 + w^2} \alpha_{tt}^{(1)} \dots \quad (11)$$

$$\dots - \frac{w^2}{t^2 + w^2} \alpha_{ww}^{(1)} - \frac{1}{2} \frac{h}{1-h} \frac{h'}{h}$$

with

$$\frac{h'}{h} = \alpha_{ww}^{(1)} - \alpha_{tt}^{(1)} - \frac{1}{2} (T_{C_{44}}^{(1)} - T_{C_{66}}^{(1)}) \dots \quad (12)$$

$$+ \frac{\pi}{2} \frac{t}{w} \sqrt{\frac{C_{44}}{C_{66}}} \left[ \alpha_{tt}^{(1)} - \alpha_{ww}^{(1)} + \frac{1}{2} (T_{C_{44}}^{(1)} - T_{C_{66}}^{(1)}) \right] \cdot A$$

and

$$A = \frac{\sum_{n=0}^{\infty} \left( \frac{1 - th^2 \left[ \frac{t(2n+1)\pi}{2w} \sqrt{\frac{C_{44}}{C_{66}}} \right]}{(2n+1)^4} \right)}{\sum_{n=0}^{\infty} \left( \frac{1}{(2n+1)^5} th \left[ \frac{t(2n+1)\pi}{2w} \sqrt{\frac{C_{44}}{C_{66}}} \right] \right)} \quad (13)$$

$T_f^{(1)}$  depends on  $C_{44}$  and  $C_{66}$  and the ratio  $w/t$ . In Fig. 5, the evolution of the first TCF versus rotated X-cut is drawn for LGT, LGS, GaPO<sub>4</sub> and Quartz. The beam has 1 mm width, 2 mm thick and 20 mm long. In this case, the ratio  $w/t$  is equal to 0.5. The temperature-compensated cut is found for quartz at  $\theta = 32^\circ$  [16]. LGS and LGT crystal have a similar behavior.

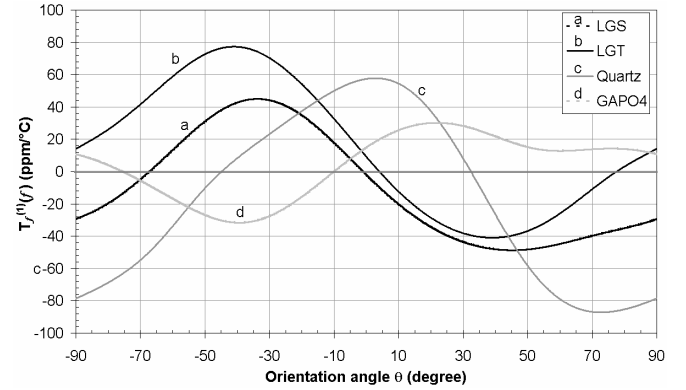


Figure 5.  $T_f^{(1)}$  versus rotation angle  $\theta$  for LGT in torsional mode,  $w/t = 0.5$ .

Table 5 sums up the values of the rotation angle for which the first order TCF is null.

TABLE V. TEMPERATURE-COMPENSATED CUTS FOR RECTANGULAR BEAMS IN QUARTZ, GAPO<sub>4</sub>, LGS AND LGT: TORSION,  $w/t = 0.5$ .

| Rectangular beam | Quartz [17]   | GaPO <sub>4</sub> [18]                               | LGS [18]  | LGT [18]  |
|------------------|---|--|---|---|
| Torsion          | $\theta = -44.8^\circ$<br>or<br>$\theta = 32.4^\circ$ | $\theta = -75.7^\circ$<br>or<br>$\theta = -10^\circ$ | $\theta = -67.2^\circ$<br>or<br>$\theta = -1.1^\circ$ | $\theta = 4.1^\circ$<br>or<br>$\theta = 77.6^\circ$ |

All materials have temperature compensated cuts. LGS and LGT present angles with  $T_f^{(1)} = 0$ . One of two cut angles for which  $T_f^{(1)}$  is null is very closed to the Y crystallographic axis.

In Fig. 6, the beam has 2 mm width, 1 mm thick and 20 mm long. The ratio  $w/t$  is equal to 2. In this case, quartz don't have temperature-compensated cut. Table 6 sums up the values of the rotation angles for which the first order TCF is null for GaPO<sub>4</sub>, LGS and LGT.

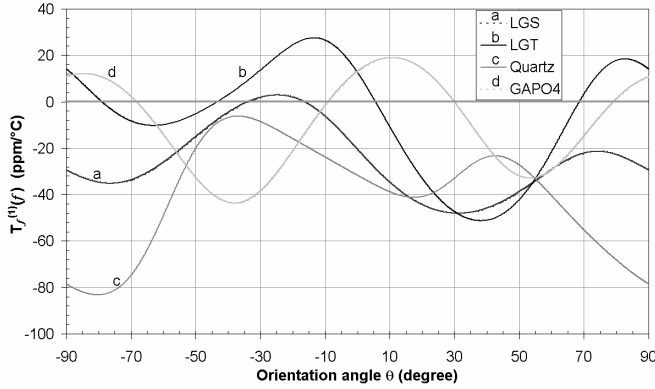


Figure 6.  $T_f^{(1)}$  versus rotation angle  $\theta$  for LGT in torsional mode,  $w/t = 2$ .

TABLE VI. TEMPERATURE-COMPENSATED CUTS FOR RECTANGULAR BEAMS IN QUARTZ, GaPO<sub>4</sub>, LGS AND LGT: TORSION,  $w/t = 2$ .

| Rectangular beam | GaPO <sub>4</sub> [18] | LGS [18]               | LGT [18]               |
|------------------|------------------------|------------------------|------------------------|
| Torsion          | $\theta = -68.4^\circ$ | $\theta = -33.9^\circ$ | $\theta = -79^\circ$   |
|                  | or                     | or                     | or                     |
|                  | $\theta = -9.1^\circ$  | $\theta = -16.5^\circ$ | $\theta = -43.4^\circ$ |
|                  | or                     |                        | or                     |
|                  | $\theta = 29.9^\circ$  |                        | $\theta = 5.6^\circ$   |
|                  | or                     |                        | or                     |
|                  | $\theta = 79.1^\circ$  |                        | $\theta = 68.5^\circ$  |

## V. CONCLUSION

First order temperature compensated cuts in LGT for extensional, flexural and torsional modes have been demonstrated theoretically. In length extension, the cut angles are  $-7.3^\circ$  and  $68.6^\circ$ . In flexion, we have  $\theta = -6.6^\circ$  and  $\theta = 69^\circ$ . About torsional mode, temperature compensated cuts can be expected around  $\theta = -67^\circ$  and  $\theta = -1^\circ$  for LGS and around  $\theta = 4^\circ$  and  $\theta = 78^\circ$  for LGT. Length extensional and flexural modes have a thermal behavior very similar. For LGS and LGT, the model does not allow to predict with confidence temperature-compensated cuts above 250 °C since the model is limited to second-order temperature effects fitted with respect to room temperature, whereas for GaPO<sub>4</sub> temperature effects have been measured up to very high temperature well above 250 °C with a third order polynomial fit.

## REFERENCES

[1] J. Bohm, R.B. Heimann, M. Hengst, R. Roewer and J. Schindler, "Czochralski growth and characterization of piezoelectric single crystals with langasite structure:  $\text{La}_3\text{Ga}_5\text{SiO}_{14}$  (LGS),  $\text{La}_3\text{Ga}_{5.5}\text{Nb}_{0.5}\text{O}_{14}$  (LGN) and  $\text{La}_3\text{Ga}_{5.5}\text{Ta}_{0.5}\text{O}_{14}$  (LGT). Part I", J. Cryst. Growth, vol. 204, n° 1-2, pp. 128-136, (1999).

[2] J. Bohm, E. Chilla, C. Flannery, H.J. Frölich, T. Hauke, R.B. Heimann, M. Hengst, and U. Straube, "Czochralski growth and characterization of piezoelectric single crystals with langasite structure:  $\text{La}_3\text{Ga}_5\text{SiO}_{14}$  (LGS),  $\text{La}_3\text{Ga}_{5.5}\text{Nb}_{0.5}\text{O}_{14}$  (LGN) and  $\text{La}_3\text{Ga}_{5.5}\text{Ta}_{0.5}\text{O}_{14}$  (LGT). II. Piezoelectric and elastic properties", J. Cryst. Growth, vol. 216, n° 1-4, pp. 293-298, (2000).

[3] H. Kong, J. Wang, H. Zhang, X. Yin, X. Cheng, Y. Lin, X. hu, X. Xu and M. Jiang, "Growth and characterization of  $\text{La}_3\text{Ga}_{5.5}\text{Ta}_{0.5}\text{O}_{14}$  crystal", Crystal research and technology, vol. 39, n° 8, pp. 686-691, (2004).

[4] J. Luo, D. Shah, C.F. Klemenz, M. Dudley and H. Chen, "The Czochralski growth of large-diameter  $\text{La}_3\text{Ga}_{5.5}\text{Ta}_{0.5}\text{O}_{14}$  crystals along different orientations", J. Cryst. Growth, vol. 287, n° 2, pp. 300-304, (2006).

[5] R.C. Smythe, R.C. Helmbold, G. E. Hague and K. A. Snow, "Langasite, Langanite, and Langatate Bulk-Wave Y-cut resonators", IEEE Trans. on Ultrason. Ferroelec. and Freq. Contr., vol. 47, no. 2, March, pp. 355-360, (2001).

[6] M. Pereira da Cunha, D.C. Malocha, E. Adler, K.J. Casey, "Surface and pseudo surface acoustic waves in langatate: predictions and measurements," IEEE Trans. on Ultrason. Ferroelec. and Freq. Contr., vol. 49, n° 9, Sept., pp. 1291-1299, (2002).

[7] J. Schreuer, "Elastic and piezoelectric properties of  $\text{La}_3\text{Ga}_5\text{SiO}_{14}$  and  $\text{LaGa}_{5.5}\text{Ta}_{0.5}\text{O}_{14}$ : an application of resonant ultrasound spectroscopy", IEEE Trans. on Ultrason. Ferroelec. and Freq. Contr., vol. 49, no. 11, Nov., pp. 1474-1479, (2002).

[8] Y.V. Pisarevski, P.A. Senyushenkov and N.A.Moiseeva, "Elastic, piezoelectric, dielectric properties of  $\text{La}_3\text{Ga}_{5.5}\text{Ta}_{0.5}\text{O}_{14}$  single crystals", ASFC, pp. 742-747, (1998).

[9] D.C. Malocha, E. Adler, S. Frederick, M. Chou, M.P. de Cunha, R.C. Smythe, R. Humbold and Y.S. Zhou, "Recent measurement of materials constants versus temperature of langate, langanite and langasite", Proc. 54th IEEE Ann. Freq. Cont. Symp., Kansas city, Missouri, 7-9 June, pp. 200-205, (2000).

[10] D.C. Malocha, H. François-Saint-Cyr, K. Richardson, R. Helmbold, "Measurements of LGS, LGN and LGT thermal coefficients of expansion and density", IEEE Trans. on Ultrason. Ferroelec. and Freq. Contr., vol. 49, no. 3, March, pp. 350-355, (2002).

[11] R. Bourquin and B. Dulmet, "New sets of data for the thermal sensitivity of elastic coefficients of langasite and langatate", in Proc. 20th European Frequency and Time Forum, Braunschweig, Germany, 27-30 March, pp. 26-32, (2006).

[12] L. Delmas, F. Sthal, E. Bigler, B. Dulmet and R. Bourquin, "Temperature-compensated cuts for length-extensional and flexural vibrating modes in GaPO<sub>4</sub> beam resonators", IEEE Trans. on Ultrason. Ferroelec. and Freq. Contr., vol. 52, no. 4, April, pp. 666-671, (2005).

[13] L. Delmas, F. Sthal, E. Bigler, J.J. Boy, S. Galliou, R. Bourquin, "Experimental study of temperature effects in vibrating beam and thickness-shear resonators of GaPO<sub>4</sub> machined by ultrasonic milling", in Proc. IEEE Int. Ultrason. Ferroelec. and Freq. Cont. 50th Anniversary Joint Conf., Montreal, Canada, 24-27 August, pp. 625-629, (2004).

[14] F. Sthal, E. Bigler, R. Bourquin, "Thermal compensation in GaPO<sub>4</sub> beam resonators: Experimental evidence for length extensional mode", IEEE Trans. on Ultrason. Ferroelec. and Freq. Contr., vol. 54, no. 1, Jan., pp. 196-197, (2007).

[15] F. Sthal, E. Bigler, J. Maisonnnet, R. Bourquin and B. Dulmet, "Langasite beam resonators: theoretical and experimental investigations", Proc. IEEE Int. Freq. Cont. Symp., Miami, Florida, 5-7 June, pp. 481-484, (2006).

[16] P. Truchot and R. Bourquin, "Torsional quartz resonators", in Proc. 8th European Frequency and Time Forum, Munchen, Germany, 9-11 March, pp. 862-871, (1994).

[17] "IRE standards on piezoelectric crystals, 1949," Proc. IRE, vol. 37, pp. 1378-1395, Dec. (1949).

[18] ANSI/IEEE Std 176-1987, "IEEE standards on piezoelectricity", (1987).